Available online at www.sciencedirect.com
ScienceDirect
Trans. Nonferrous Met. Soc. China 29(2019) 931−940
Transactions of Nonferrous Metals Society of China
www.tnmsc.cn

Effect of ECAP on microstructure and tensile properties of A390 aluminum alloy

Esmaeil DAMAVANDI, Salman NOUROUZI, Sayed Mahmood RABIEE, Roohollah JAMAATI

Department of Materials Engineering, Babol Noshirvani University of Technology, Shariati Ave., Babol 47148–71167, Iran

Received 24 July 2018; accepted 14 January 2019

Abstract: The purpose of the present research is to determine the tensile strength and elongation of the A390 alloy processed by ECAP and to reveal the relationship between the microstructure and tensile properties. Optical microscopy (OM), scanning electron microscopy (SEM) and energy dispersive spectroscopy (EDS) were used for microstructural analysis of the samples. The results of the mechanical testing showed that the ultimate tensile strength (UTS) increased from 142 MPa for the as-cast sample to 275 MPa for the sample after the third ECAP pass. Increasing the ECAP passes up to 4 led to a remarkable enhancement of elongation compared with the as-cast sample. It was found that the improvement of strength and ductility of A390 alloy with increasing the number of ECAP passes was attributed to the homogenous distribution of particles, reduction of particle size, and elimination of voids especially adjacent to the primary silicon particles. The results of fractography demonstrated that when the number of ECAP passes increased to 4, the uniform round dimples formed and the relatively brittle as-cast sample transformed to a ductile alloy.
Key words: aluminum alloy; equal channel angular pressing; microstructure; tensile properties

1 Introduction

Hypereutectic Al−Si alloys such as A390 are widely used for castings in industries, since they have a low coefficient of thermal expansion, high hardness and wear resistance, high tensile strength at elevated temperatures, and good castability [1,2]. However, the toughness of these alloys is low. Some researchers [3−5] have reported that the mechanical properties of Al−Si alloys are influenced by the size, morphology, and distribution of the primary and eutectic silicon. In fact, the distribution of coarse primary Si particle in hypereutectic Al−Si alloys mainly contributes to stress concentration, crack initiation, and propagation during the actual service condition. MA et al [1] have reported that the impact toughness of hypereutectic Al−Si alloys is related to eutectic silicon shapes, dendrite arm spacing of Al matrix, other intermetallic components, primary silicon particles, and casting defects such as porosity. In these alloys, cracks create and propagate easily at the particle−matrix interfaces, resulting in a brittle fracture. Therefore, the size and morphology of silicon particles (both primary and eutectic) have a significant effect on the toughness. In addition, the presence of fine grains with high angle grain boundaries (HAGBs) plays an important role in the impact toughness. The improved impact toughness is influenced by the ductile aluminum alloy matrix.

To improve the microstructures of alloys, there are several methods such as rapid solidification [6], heat treatment [7], and plastic deformation [8]. YU et al [9] have investigated the influence of T6 heat treatment on the fracture behavior of hypereutectic Al−Si alloy. The results showed that T6 treatment led to the improvement of the mechanical properties of A390 alloy due to the transformation of plate-like eutectic Si particles into granular particles and dissolution of Al_2Cu into Al matrix. PIATKOWSKI et al [10] have studied the influence of melt overheating temperature on the crystallization parameters and primary structure of A390 alloy. It was found that the degree of overheating influences the microstructural evolution and morphologies of primary silicon of the Al−Si alloys.

Nowadays, severe plastic deformation (SPD) is used for refining microstructure of metallic materials [11−13]. Equal channel angular pressing (ECAP) is one of the most employed SPD methods which could obtain special mechanical advantages without considerably changing

Corresponding author: Salman NOUROUZI; E-mail: s-nourouzi@nit.ac.ir
DOI: 10.1016/S1003-6326(19)65002-8

the geometries of metals [14,15]. NISHIDA et al [16] have modified ECAP for continuous processing without the return of samples and named it the rotary-die equal channel angular pressing (RD-ECAP). They have investigated the effects of RD-ECAP on impact toughness of Al−11%Si eutectic alloy. The ultrafine grain with high angle grain boundaries (HAGBs) and high content of fine silicon particles was necessary for attaining high absorbed energy at Charpy impact testing. The coarse Al grains and primary Si particles in the hypereutectic Al−Si alloy are drastically refined via ECAP as reported by JIANG et al [17]. After ECAP process, the primary Si crystals broke and some voids formed around them. With increasing the number of ECAP passes, the size of Si particles decreased and the voids almost eliminated. CARDOSO et al [18] have used pre-heat treatment and extrusion before ECAP process for Al−10%Si alloy. All processing treatments lead to refinement of Si particles and matrix grain, with corresponding improvement in toughness.

With regard to other researches, the influence of ECAP on the strength and elongation of A390 alloy was not reported. Therefore, the aim of the present work is to determine the tensile strength and elongation of the A390 alloy processed by ECAP and to reveal the relationship between the microstructure and tensile properties. The study includes quantitative analysis by Clemex software and the examination of the influence of ECAP passes on the microstructure, mechanical properties, and fracture surface of samples.

2 Experimental

The alloy used in the present study was the as-cast A390 aluminum alloy. The chemical composition of A390 alloy is presented in Table 1.

Table 1 Chemical composition of A390 aluminum alloy (wt.%)

Si	Cu	Mg	Fe	Mn	Zn	Cr	Al
18.00	4.20	0.31	0.64	0.29	0.06	0.02	Bal.

Circular billets with a diameter of 12 mm and a length of 60 mm were machined from the as-cast material and processed by ECAP. The ECAP die had a circular cross-section channel with a diameter of 12 mm, an inner corner angle, ϕ, of 110° and an outer corner angle, Ψ, of 70°. The material chosen for the die was the D3 tool steel. Before each ECAP pass, the billet was pre-heated at 300 °C for 15 min. Then, it was processed by 4 ECAP passes, using route A at 400 °C with a punch speed of 1 mm/s. A mixed lubricant of molybdenum disulfide (MoS_2) and graphite was used to reduce friction between the die wall and the billet.

After ECAP process, tensile samples were machined with the tensile axis aligned to the longitudinal direction. The tensile tests were performed at room temperature according to ASTM-E9 standard. The gauge diameter and length of the tensile test samples were 4 and 16 mm, respectively. Each test was repeated twice to access accuracy in results. Tensile tests were performed at a strain rate of 2×10^{-3} s^{-1}.

For metallographic preparation, the samples were cut along the cross-section, followed by grinding on SiC paper and finally mechanical polishing with the 0.25 μm diamond paste. The optical microscopy (OM) and scanning electron microscopy (SEM) were used for microstructure and fractography studies. The average particle size and sphericity of primary Si and eutectic Si were analyzed by image analysis software.

3 Results and discussion

3.1 Microstructure

The optical micrograph of the as-cast A390 alloy is shown in Fig. 1(a). The as-cast sample consists of primary silicon particles (PSPs), Al–Si eutectic, and some intermetallic compounds. As shown in this figure, the PSPs have polygonal, triangle and thick plate morphologies. Also, aluminum dendrites are clearly observed. Actually, Si discharge around primary particles in the melt before pouring starts is believed to be responsible for the shift in local chemistry which simplifies the formation of aluminum dendrites.

SEM observations and EDS analysis were performed in order to determine the chemical composition of intermetallic compounds (Figs. 1(b−f)). Regarding the peaks in EDS analysis and according to the results in Refs. [19,20], the three main intermetallic compounds include β-Al_5FeSi (needle-shaped), $Al_{15}(FeMn)_3Si_2$ (script-like), and Al_2Cu (interconnected with each other and agglomerated severely). In fact, because of the low solubility of iron in aluminum, almost all the iron atoms form intermetallic compounds. IRIZALP and SAKLAKOGLU [20] have found that the brittle and needle-like morphology of β-Al_5FeSi leads to a reduction of the tensile strength and elongation. HAGHSHENAS and JAMALI [3] expressed that the Fe-rich phases tend to have a relatively low bond strength due to their hard and brittle nature.

Figure 2 shows the OM images of the samples processed by ECAP. As shown in Fig. 2(a), the dendritic structure is decreased after the first ECAP pass. With increasing number of passes up to 4, no dendritic structure is found in the alloy. On the other hand, it is observed that ECAP process can break PSPs and form voids around them because of the brittle nature of the silicon crystals (white arrows). Other researchers [21,22]

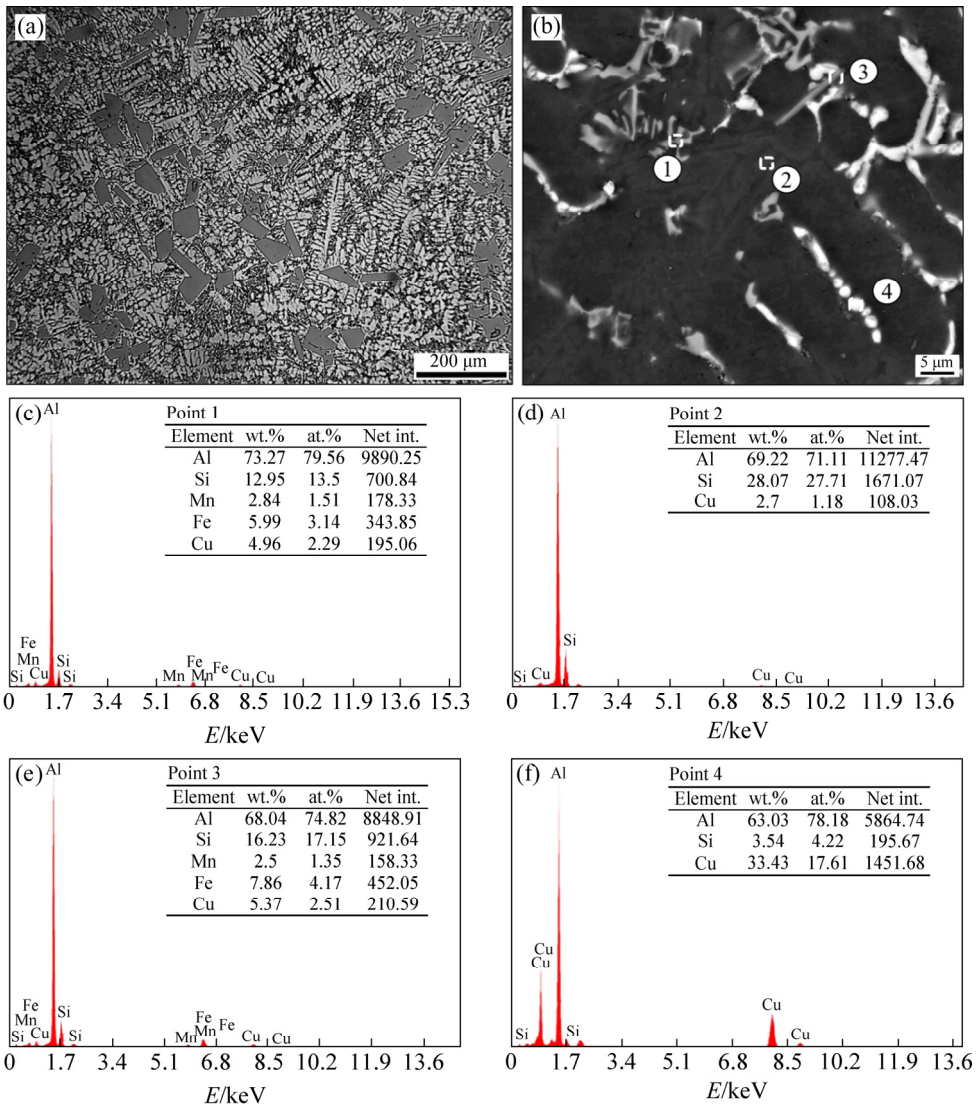

Fig. 1 OM (a) and SEM (b) images with EDS spectra (c−f) of as-cast sample

have verified the formation of voids around the PSPs after plastic deformation. Also, with increasing the number of passes, the pre-formed voids around the PSPs were eliminated or the size of voids deceased due to the flowing of Al matrix. But, after 4 passes, some voids remained, yet. According to Fig. 2, the average size of the PSPs is gradually decreased due to the breakage of PSPs with increasing the number of passes.

The size and sphericity distributions of the PSPs in different conditions are illustrated in Fig. 3. It is seen that the PSPs size in the as-cast sample (green line) is very scattered. It may be dependent on casting conditions and nature of PSPs in solidification moment. It is noteworthy that the fractions of PSPs larger than 50 μm in the as-cast, 1, 2, 3, and 4 passes processed samples are 30%, 18%, 6%, 5%, and 3%, respectively. On the other hand, the fractions of PSPs less than 30 μm in the as-cast, 1, 2, 3 and 4 passes processed samples are 28%, 50%, 62%, 66%, and 74%, respectively. Nevertheless, further increasing the number of passes up to 4 leads to the decrease in the average size of PSPs. The average sphericity of PSPs of the as-cast alloy is about 0.62 and the sphericity distribution is uneven due to irregular morphologies such as polygons, star-shaped and thick plates with sharp edges in the primary silicon. With increasing number of ECAP passes, the PSPs are broken (see Fig. 2). As a result of fragmentation of PSPs, as shown in Fig. 3(b), the sphericity value increases. It should be noted that increasing the sphericity of PSPs leads to decreasing the stress concentration at particle/matrix interfaces. JUNG et al [23] also reported that the spheroidization of Si reduces the stress concentration at the interface between silicon particles and the aluminum matrix.

Figure 4 shows the microstructures of as-cast and ECAP-processed samples at a higher magnification. Figure 4(a) shows the continuous networks of lengthy- and acicular-shaped eutectic silicon particles (ESPs) and

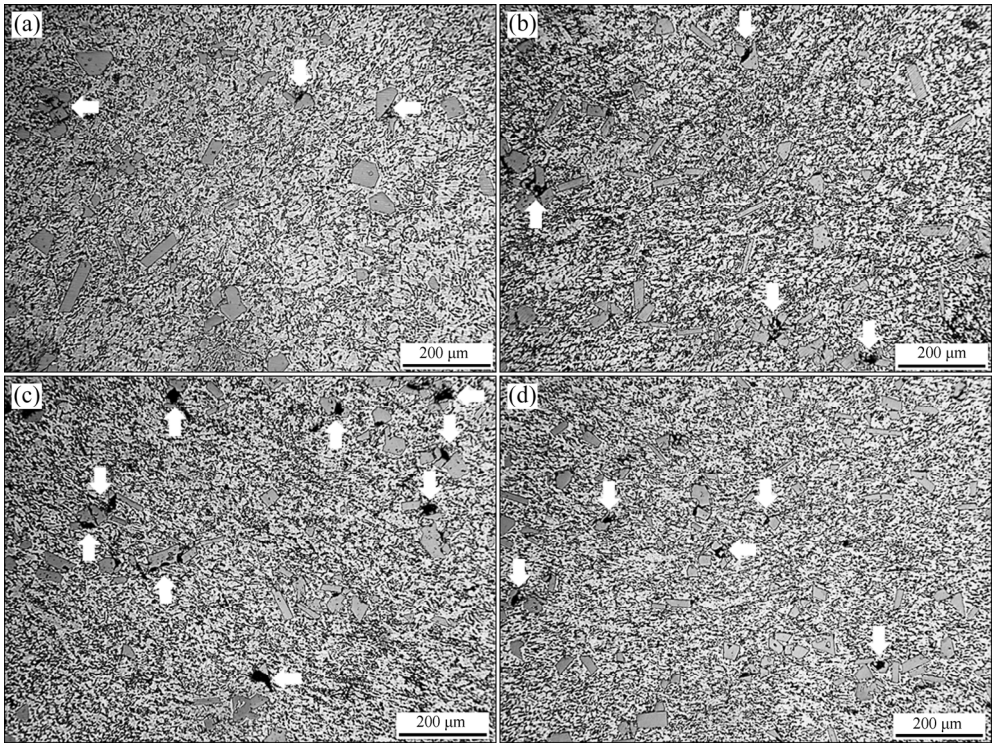

Fig. 2 OM images of ECAP-processed samples with different passes: (a) 1 pass; (b) 2 passes; (c) 3 passes; (d) 4 passes

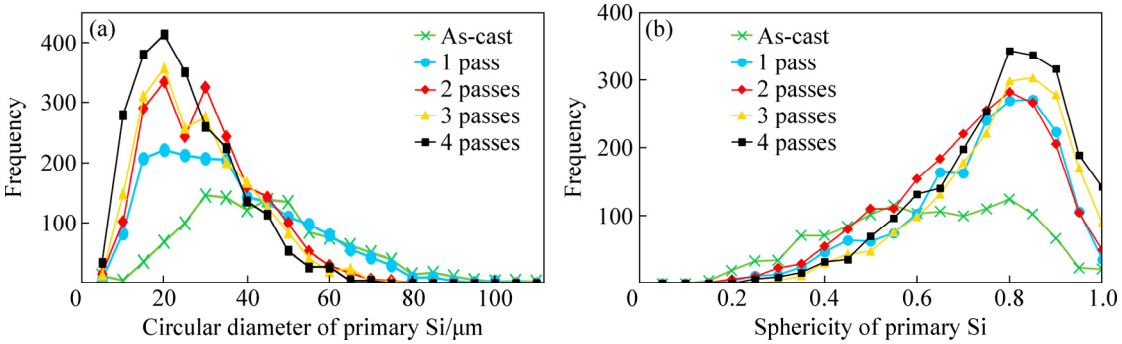

Fig. 3 Size (a) and sphericity (b) distributions of PSPs under different conditions

some connected intermetallic compounds (white rectangles). According to Figs. 4(b−e), during ECAP processing, many ESPs and intermetallic compounds are broken and separated. In addition, compared with the as-cast alloy, the ECAP process leads to uniform dispersion of the ESPs and the intermetallic compounds in the aluminum matrix.

For fragmentation of silicon particles under the thermomechanical condition, there are two distinct mechanisms including mechanical fragmentation and thermal disintegration as reported by HAGHDADI et al [24]. As shown in Figs. 2 and 4, PSPs were mechanically fragmented and there was no sign of necking in the silicon particles. Actually, the stresses resulting from plastic deformation of the matrix (during ECAP process, the aluminum matrix undergoes a higher flow stress level) would cause particle fragmentation. These stresses may be results of the differences in elastic modulus and deformation behavior of silicon particles and aluminum matrix. Also, since the ECAP process was performed at high temperature and samples were held in ECAP die during deformation, the mismatch of thermal expansion coefficients between the silicon and aluminum leads to creating a high degree of local stresses between particles and matrix [25]. The effect of imposed ECAP passes on the aspect ratio and size of ESPs as well as the related features in the as-cast sample is presented in Fig. 5. It can be seen that the aspect ratio and size of ESPs are strongly affected by ECAP passes. The aspect ratio of ESPs is decreased with increasing the number of passes. The average aspect ratio of ESPs is decreased from 4.1 for the as-cast sample to 2.7 after the fourth pass. In addition, the fractions of ESPs larger than 5 μm in the as-cast, 1, 2, 3 and 4 passes processed samples are

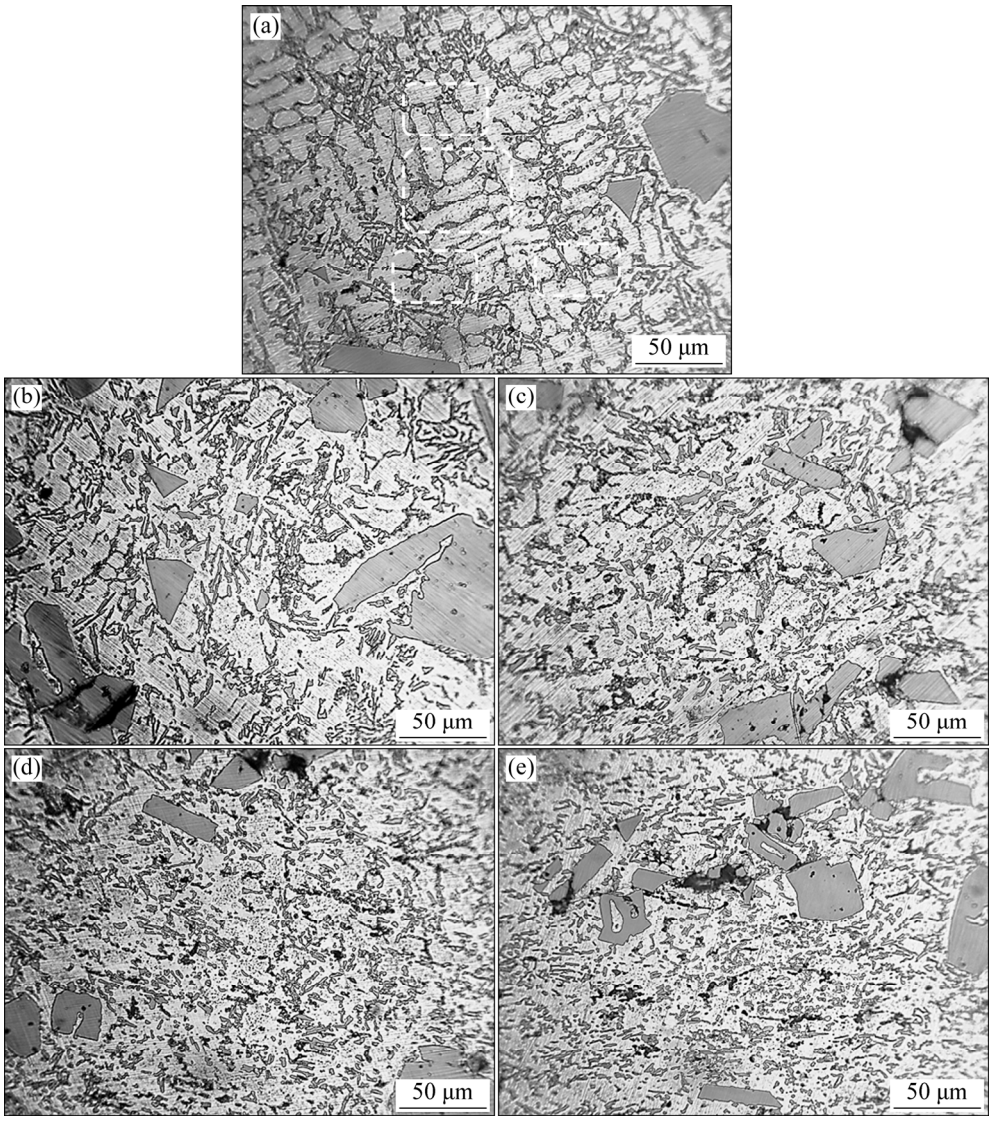

Fig. 4 High magnification optical microscopy images of as-cast (a), 1 (b), 2 (c), 3 (d) and 4 (e) ECAP passes processed samples

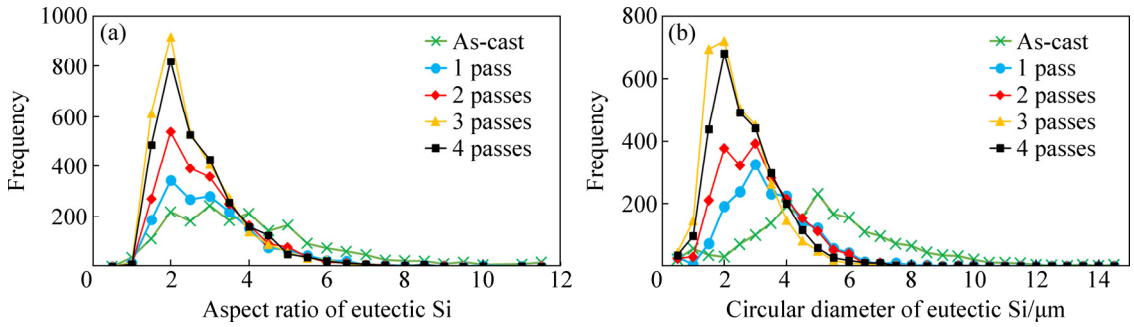

Fig. 5 Aspect ratio (a) and size (b) distributions of ESPs under different conditions

46%, 9%, 5%, 1%, and 3%, respectively. In a similar way, the fractions of ESPs less than 2 μm in the as-cast, 1, 2, 3 and 4 passes processed samples are 8%, 17%, 29%, 51%, and 43%, respectively. It is clear that a large number of coarse eutectic silicon is fragmented in first two ECAP passes.

The mean sizes of ESPs in the as-cast and 1, 2, 3, and 4 passes processed samples are 5.3, 3.4, 3.1, 2.4 and 2.7 μm, respectively. The size of ESPs after the fourth pass is slightly higher than that of ESPs after the third pass. This may be related to diffusion phenomena. After the third ECAP pass, the uniform distribution of very fine ESPs leads to decreasing the distance between the particles. The short distance between particles

accompanied with high temperature and mechanical working can facilitate the movement of atoms. On the other hand, it can be said that decreasing the size of particles leads to increasing the dislocation density during the fourth cycle and thus more atoms are stimulated for diffusion.

3.2 Tensile properties

Engineering stress−engineering strain curves of the as-cast and the ECAP-processed samples are shown in Fig. 6.

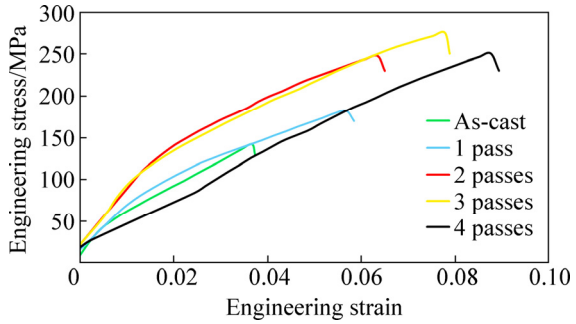

Fig. 6 Engineering stress−engineering strain curves of various samples

According to Fig. 6, the minimum ultimate tensile strength (UTS) and elongation are obtained for the as-cast sample. This is due to the presence of large PSPs, dendrite structure, coarse and continuous intermetallic compounds, and networks of platelet eutectic silicon in the as-cast sample. Ductility and strength are the main mechanical properties of any material but these properties generally have opposing specifications. So, materials may be ductile or strong but they are rarely both [26]. As shown in Fig. 6, however, both tensile strength and elongation of the A390 alloy increased via ECAP process. The UTS and the elongation of the sample increased from 142 MPa and 3% (for the as-cast sample) to 182 MPa and 6% (after the first pass), respectively. It can be observed that the UTS of the second pass is 36% higher than that of the first ECAP pass sample. In the first two passes of ECAP process, as shown in Figs. 2−4, some PSPs were broken and the size of them was decreased. On the other hand, the connection between the eutectic silicon networks is partly interrupted and the size of them was decreased. The dendritic structure of aluminum matrix was modified to the non-dendritic structure. Among the ECAP-processed samples, three ECAP passes proessed sample shows the maximum UTS with an increase of 93% compared with the as-cast sample. The formation of a non-dendritic structure and a reduced grain size, a better distribution of silicon particles in the Al matrix, and the presence of fine ESPs and intermetallic compounds are the most important factors which lead to obtaining the excellent value of UTS for the sample after the third pass. The processed samples show an increase in the elongation of about 200%, from 3% for the as-cast sample to about 9% for the fourth ECAP pass sample. YOON et al [27] have reported that the small size of silicon particles is the main cause of the high ductility of the hypereutectic Al−Si alloys. It has been made sure that the A390 alloy after ECAP at elevated temperatures exhibits higher elongation with increasing the number of ECAP passes. Interestingly, after the fourth pass, the size and aspect ratio of EPSs in the alloy slightly increased compared with the sample after the third pass. This is owing to decreasing the PSPs size, more homogenous distribution of particles in the matrix, eliminating the voids adjacent to the PSPs, and grain refinement of aluminum. MA et al [28] expressed that the grain refinement of Al matrix, when the size of particles does not change greatly, is one of the major parameters to increase the impact toughness of Al−11%Si alloy.

3.3 Fractography

Figure 7 shows the fracture surface of the as-cast sample and corresponding EDS analysis. According to this figure, there are many PSPs on the fracture surface. The breakage of PSPs is observed in many places as indicated by red arrows. It can be said that, during the tensile test, the PSPs are fractured owing to their brittle nature. All PSPs exhibited a cleavage fracture as indicated by white arrows. The fractograph and the EDS analysis of fracture surface indicated that the cracks tend to pass through the PSPs and networks of eutectic compounds. It is clear that this is a brittle fracture. In brittle fracture, cracks may spread rapidly, with very small plastic deformation (see Fig. 6). IMMANUEL and PANIGRAHI [29] have reported that in the Al−Si alloy, porosity, particles/matrix interface, and sharp edges of particles are potential sites for crack initiation because these are the stress risers. It should be noted that the mode of fracture is extremely related to the mechanism of crack propagation [30].

Figure 8 shows SEM fractographs for the fracture surfaces of as-cast and ECAP-processed samples. As seen in Fig. 8(a), some PSPs are separated from the aluminum matrix as indicated by yellow arrows. From Fig. 8(b), it is observed that the unmodified acicular ESPs may be the source of crack nucleation (see red arrows). Actually, the weak Si particle/Al matrix interfaces and the unmodified acicular ESPs raise the stress and thus crack nucleation.

Figure 8(c) depicts the fracture surface of the first ECAP pass sample. It can be seen that the size and the sharp edges of PSPs are slightly decreased and there are

more dimples (as indicated by red arrows) compared with the as-cast sample. However, according to Fig. 8(d), brittle fracture is the main fracture mechanism for the first ECAP pass sample. With increasing the number of passes up to 2, as shown in Figs. 8(e) and (f), the number of cracked PSPs and also dimples (as indicated by white arrows) increased. With regard to Fig. 8(f), it is clear that some regions of fracture surface do not have any dimples (red rectangles). According to the stress−strain curve and the presence of both brittle features and dimples, it can be concluded that the fracture mode is mixed (i.e. a combination of both brittle and ductile fracture). Figure 8(g) shows the fracture surface of the three ECAP passes sample in which a large number of micro dimples are seen. Good bonding between some PSPs and aluminum matrix is observed in Fig. 8(h) (red arrows). The fracture surface of the three ECAP passes sample is filled by dimples with different sizes. It is clear that the mechanism of fracture is changed to ductile fracture. In fact, the ductile fracture is specified by wide plastic deformation (see Fig. 6) in the vicinity of an advancing crack. The important characteristic of this fracture type is the presence of dimples or microvoids on the fracture surface. The presence of a large number of dimples, good bonding between PSPs and matrix, and also the fine sphere-like ESPs led to obtaining the best tensile properties after the third ECAP pass. Finally, as shown in Fig. 8(i), PSPs are well covered by the matrix. The white arrows in Fig. 8(j) indicate the high quality of bonding between the Si particles and the surrounding Al matrix, while two cracks take place within the PSPs due to brittle nature of silicon crystals (black ellipse). The fourth ECAP pass leads to intense damage of the PSPs with several slip traces and cracks (black ellipse). It can also be observed that with increasing number of passes and decreasing size and aspect ratio of ESPs, the uniform

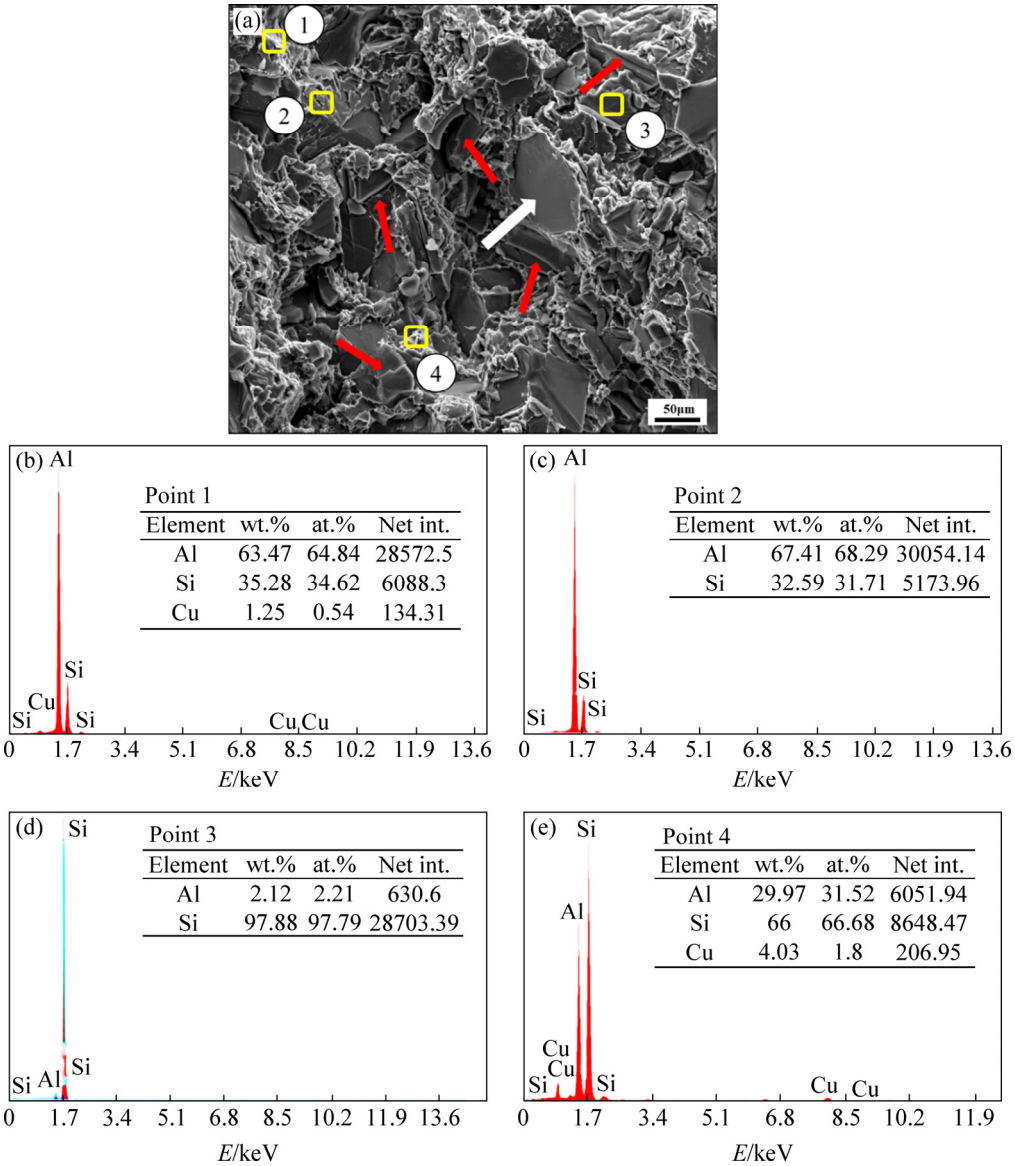

Fig. 7 High magnification fractograph (a) with EDS analysis (b−e) of as-cast sample

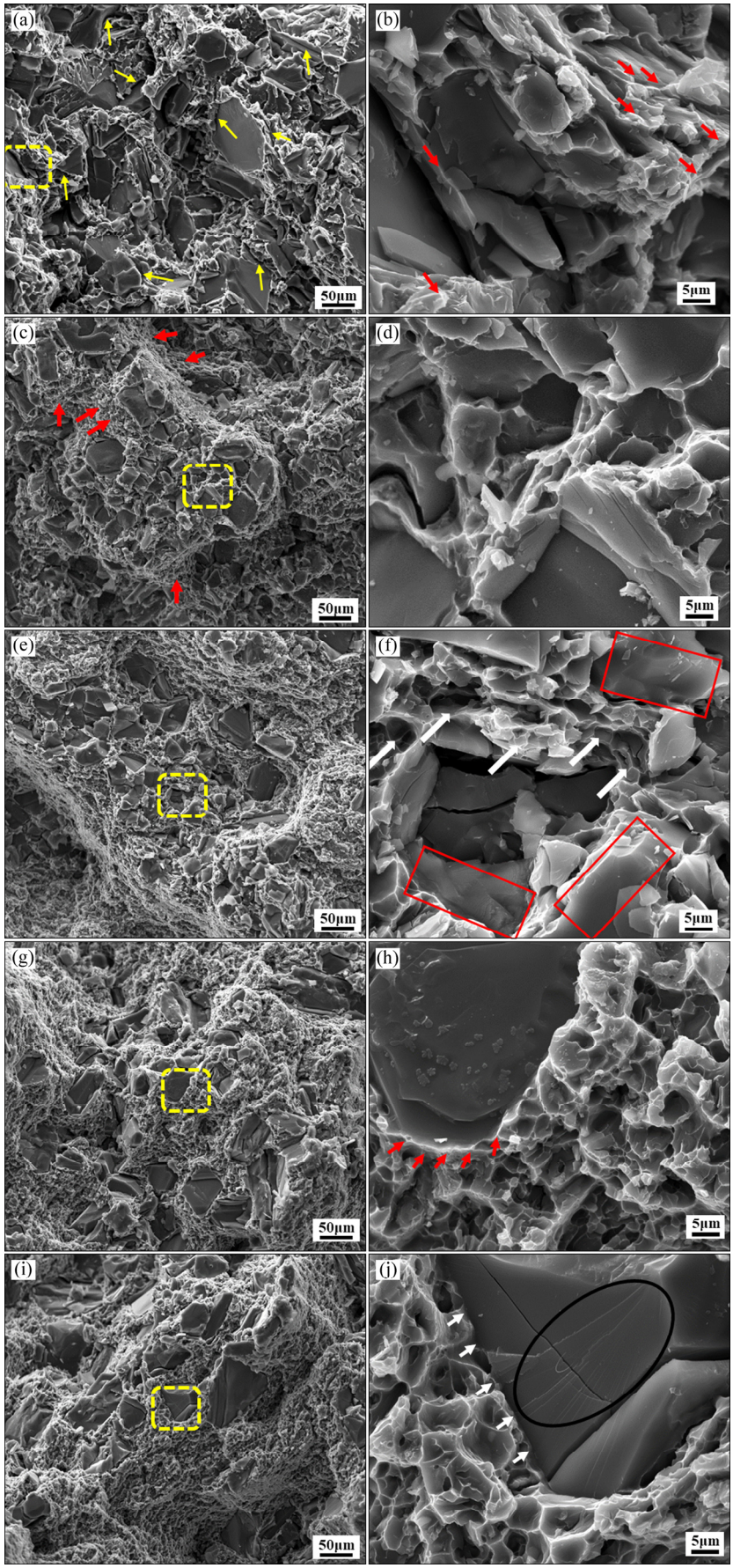

Fig. 8 SEM fractographs showing fracture surfaces of different samples: (a, b) As-cast; (c, d) 1 ECAP pass; (e, f) 2 ECAP passes; (g, h) 3 ECAP passes; (i, j) 4 ECAP passes

round dimples are formed. In fact, a large number of small dimples indicate a complete ductile fracture in the aluminum matrix.

4 Conclusions

(1) ECAP process led to complete elimination of the dendritic structure of the as-cast A390 alloy sample, reduction of particle size, and better dispersion of particles in the aluminum matrix.

(2) The maximum UTS and elongation values were obtained after third and fourth passes, respectively. The improvement in the tensile strength and elongation was attributed to the grain refinement, homogeneous distribution of PSPs, and intermetallic compounds, and also good bonding between PSPs and aluminum matrix.

(3) Fractography studies revealed that the brittle fracture is the main fracture mechanism in the as-cast sample due to the presence of the coarse PSPs with sharp edges, the networks of unmodified lengthy acicular ESPs and intermetallic compounds, and weak silicon/ aluminum interface.

(4) With increasing the number of ECAP passes, the fracture mechanism changed from brittle fracture to ductile one.

(5) The behavior of A390 alloy after the fourth ECAP pass turned to a perfect ductile fracture. In fact, the stress concentration sites after the fourth pass dramatically decreased compared with that of the as-cast sample. Therefore, the elongation of alloy increased remarkably.

Acknowledgments

The authors acknowledge the funding support of Babol Noshirvani University of Technology through Grant program No. BNUT/370725/98, BNUT/370388/98, and BNUT/393044/98.

References

[1] MA A, SUZUKI K, SAITO N, NISHIDA Y, TAKAGI M, SHIGEMATSU I. Impact toughness of an ingot hypereutectic Al−23mass% Si alloy improved by rotary-die equal-channel angular pressing [J]. Materials Science and Engineering A, 2005, 399: 181−189.

[2] ZHAO J, WU S. Microstructure and mechanical properties of rheo-diecasted A390 alloy [J]. Transactions of Nonferrous Metals Society of China, 2010, 20(s3): s754−s757.

[3] HAGHSHENAS M, JAMALI J. Assessment of circumferential cracks in hypereutectic Al−Si clutch housings [J]. Case Studies in Engineering Failure Analysis, 2017, 8: 11−20.

[4] HUANG Z, WANG K, ZHANG Z, LI B, XUE H, YANG D. Effects of Mg content on primary Mg_2Si phase in hypereutectic Al−Si alloys [J]. Transactions of Nonferrous Metals Society of China, 2015, 25: 3197−3203.

[5] KANG N, CODDET P, LIAO H, BAUR T, CODDET C. Wear behavior and microstructure of hypereutectic Al−Si alloys prepared by selective laser melting [J]. Applied Surface Science, 2016, 378: 142−149.

[6] CHEN C M, YANG C C, CHAO C G. A novel method for net-shape forming of hypereutectic Al−Si alloys by thixocasting with powder preforms [J]. Journal of Materials Processing Technology, 2005, 167(1): 103−109.

[7] LI B, ZHANG Z, WANG Z, XU J, ZHU Q. Effect of heat treatment on microstructure and mechanical properties of A390 alloy [J]. Advanced Materials Research, 2013, 652−654: 1049−1053.

[8] SPUSKANYUK V, BEREZINA A, DUBODELOV V, DAVYDENKO O, FIKSSEN V, SLIVA K. Structural modification of hypereutectic Al−16.5mass%Si alloy by thermo-mechanical treatment with ECAP [J]. Materials Science and Metallurgy Engineering, 2014, 2: 35−40.

[9] YU W, ZHAO H, WANG L, GUO Z, XIONG S. The influence of T6 treatment on fracture behavior of hypereutectic Al−Si HPDC casting alloy [J]. Journal of Alloys and Compounds, 2018, 731: 444−451.

[10] PIĄTKOWSKI J, GAJDZIK B, MATUŁA T. Crystallization and structure of cast A390 alloy with melt overheating temperature [J]. Metalurgija, 2012, 51(3): 321−324.

[11] BRYŁA K, MORGIEL J, FARYNA M, EDALATI K, HORITA Z. Effect of high-pressure torsion on grain refinement, strength enhancement and uniform ductility of EZ magnesium alloy [J]. Materials Letters, 2018, 212: 323−326.

[12] JAMAATI R, TOROGHINEJAD M R, AMIRKHANLOU S, EDRIS H. Production of nanograin microstructure in steel nanocomposite [J]. Materials Science and Engineering A, 2015, 638: 143−151.

[13] WANG Y L, LAPOVOK R, WANG J T, QI Y S, ESTRIN Y. Thermal behavior of copper processed by ECAP with and without back pressure [J]. Materials Science and Engineering A, 2015, 628: 21−29.

[14] MOGUCHEVA A, BABICH E, OVSYANNIKOV B, KAIBYSHEV R. Microstructural evolution in a 5024 aluminum alloy processed by ECAP with and without back pressure [J]. Materials Science and Engineering A, 2013, 560: 178−192.

[15] SITDIKOV O, AVTOKRATOVA E, SAKAI T. Microstructural and texture changes during equal channel angular pressing of an Al−Mg−Sc alloy [J]. Journal of Alloys and Compounds, 2015, 648: 195−204.

[16] NISHIDA Y, JIANG J, SAITO N, SHIGEMATSU I, WATAZU A. Deformation mechanism at impact test of Al−11%Si alloy processed by equal-channel angular pressing with rotary die [J]. Transactions of Nonferrous Metals Society of China, 2007, 17: 104−109.

[17] JIANG J, SHI J, YAO Y H, MA A, SONG D, YANG D. Dynamic compression properties of an ultrafine-grained Al−26wt.%Si alloy fabricated by equal-channel angular pressing [J]. Journal of Materials Engineering and Performance, 2015, 24(5): 2016−2024.

[18] CARDOSO K R, MUNOZ-MORRIS M, LEÓN K V, MORRIS D G. Room and high temperature ECAP processing of Al−10% Si alloy [J]. Materials Science and Engineering A, 2013, 587: 387−396.

[19] CHANDRA K, KAIN V. Brittle failure of hypereutectic Al−Si alloy component [J]. Journal of Failure Analysis and Prevention, 2015, 15(5): 679−685.

[20] IRIZALP S G, SAKLAKOGLU N. Effect of Fe-rich intermetallics on the microstructure and mechanical properties of thixoformed A380 aluminum alloy [J]. Engineering Science and Technology, 2014, 17(2): 58−62.

[21] JIANG J H, DAN S, SAITO N, YUAN Y, NISHIDA Y. Corrosion behavior of hypereutectic Al−23%Si alloy (AC9A) processed by severe plastic deformation [J]. Transactions of Nonferrous Metals Society of China, 2010, 20: 195−200.

[22] MA A, SUZUKI K, SAITO N, NISHIDA Y, TAKAGI M, SHIGEMATSU I. Impact toughness of an ingot hypereutectic Al−23mass%Si alloy improved by rotary-die equal-channel angular pressing [J]. Materials Science and Engineering A, 2005, 399: 181−189.

[23] JUNG J G, LEE J M, CHO Y H, YOON W H. Combined effects of ultrasonic melt treatment, Si addition and solution treatment on the microstructure and tensile properties of multicomponent AlSi alloys [J]. Journal of Alloys and Compounds, 2017, 693: 201−210.
[24] HAGHDADI N, ZAREI-HANZAKI A, ABEDI H R, SABOKPA O. The effect of thermomechanical parameters on the eutectic silicon characteristics in a non-modified cast A356 aluminum alloy [J]. Materials Science and Engineering A, 2012, 549: 93−99.
[25] NOUROUZI S, DAMAVANDI E, RABIEE S M. Microstructural and mechanical properties of Al−Al_2O_3 composites focus on experimental techniques [J]. International Journal of Microstructure and Materials Properties, 2016, 11(5): 383−398.
[26] VALIEV R Z, LANGDON T G. Principles of equal-channel angular pressing as a processing tool for grain refinement [J]. Progress in Materials Science, 2006, 51(7): 881−981.
[27] YOON S C, HONG S J, HONG S I, KIM H S. Mechanical properties of equal channel angular pressed powder extrudates of a rapidly solidified hypereutectic Al−20wt%Si alloy [J]. Materials Science and Engineering A, 2007, 449: 966−970.
[28] MA A, SAITO N, SHIGEMATSU I, SUZUKI K, TAKAGI M, NISHIDA Y. Effect of heat treatment on impact toughness of aluminum silicon eutectic alloy processed by rotary-die equal-channel angular pressing [J]. Materials Transactions, 2004, 45(2): 399−402.
[29] IMMANUEL R J, PANIGRAHI S K. Influence of cryorolling on microstructure and mechanical properties of a cast hypoeutectic Al−Si alloy [J]. Materials Science and Engineering A, 2015, 640: 424−435.
[30] CALLISTER W D. Materials science and engineering: An introduction [M]. Amsterdam: Elsevier, 1987.

ECAP 对 A390 铝合金显微组织和拉伸性能的影响

Esmaeil DAMAVANDI, Salman NOUROUZI, Sayed Mahmood RABIEE, Roohollah JAMAATI

Department of Materials Engineering, Babol Noshirvani University of Technology,
Shariati Ave., Babol 47148–71167, Iran

摘　要：研究等径角挤压(ECAP) A390 铝合金的抗拉强度和伸长率，揭示其显微组织和拉伸性能之间的关系。采用光学显微镜(OM)、扫描电镜(SEM)和能谱仪(EDS)对样品的显微组织进行分析。力学性能测试结果表明，经过 3 道次挤压后，材料的极限抗拉强度(UTS)从铸态的 142 MPa 提高到 275 MPa。与铸态样品相比，当 ECAP 道次增加到 4 时，材料的伸长率显著提高。研究发现，随着 ECAP 道次的增加，材料的强度和伸长率提高，这是因为颗粒的均匀分布、颗粒尺寸的减小和空位的消除，尤其是与原始硅颗粒相邻的空位的消除。断口分析结果表明，当 ECAP 的道次增加到 4 时，在合金中形成均匀的圆形韧窝，合金断裂机理由铸态时的脆性断裂转变为韧性断裂。

关键词：铝合金；等径角挤压；显微组织；拉伸性能

(Edited by Wei-ping CHEN)